# Photoelectron spectroscopy and theoretical studies of $[\mathrm{Co}_m(\text{pyrene})_n]^-$ ($m=1,2$ and $n=1,2$) complexes

Anil K. Kandalam,[1,a] Puru Jena,[2] Xiang Li,[3] Soren N. Eustis,[3] and Kit H. Bowen[3,a]

[1]*Department of Physics, McNeese State University, Lake Charles, Louisiana 70609, USA*
[2]*Physics Department, Virginia Commonwealth University, Richmond, Virginia 23284, USA*
[3]*Departments of Chemistry and Materials Science, Johns Hopkins University, Baltimore, Maryland 21218, USA*

Anion photoelectron spectroscopic experiments and density functional theory based calculations have been used to investigate the structural, electronic, and magnetic properties of neutral and anionic $[\mathrm{Co}_m(\text{pyrene})_n]$ ($m,n=1-2$) complexes. The calculated electron affinities and vertical transition energies of $\mathrm{Co}_m(\text{pyrene})_n$ are in good agreement with the measured values. Our results provide clear evidence for dimerization of Co atoms and formation of sandwich structures in these complexes. While the calculated spin magnetic moments of neutral $\mathrm{Co}_2(\text{pyrene})_n$ complexes suggest a preference for ferromagnetic coupling between Co atoms, the spin magnetic moment of Co atom in $\mathrm{Co}(\text{pyrene})$ and $\mathrm{Co}(\text{pyrene})_2$ complexes was reduced to $1\mu_B$. © *2008 American Institute of Physics*. [DOI: 10.1063/1.2982786]

## I. INTRODUCTION

The study of organometallics is an important field in chemistry. In the past decade, however, gas-phase metal-organic complexes, containing various organic molecules such as benzene, cyclooctatetraene, pyrene, and coronene, have attracted considerable attention. In particular, transition metal (TM)–organic complexes have been of a great interest because of the wide variety of structural and magnetic properties exhibited by them. It is well known that TM clusters have larger per atom magnetic moments than in their corresponding bulk states,[1] and these magnetic moments can further be modified when TM atoms and/or clusters interact with organic host substrates. Therefore, identifying combinations of TM atoms/clusters and organic supports, which permit the high magnetic moments of these metal clusters to be retained, would be a significant step toward discovering building blocks for novel magnetic materials.

The advent of laser vaporization techniques combined with potential applications of TM-organic complexes has resulted in numerous gas-phase experimental[2–55] as well as several theoretical studies[12,23,47,50,56–68] of these complexes. Especially, the geometrical, electronic, and magnetic properties of TM-benzene complexes have been investigated by several experimental[15,28,54,55] and theoretical[56–60,62–68] groups. Recently, TM-polycyclic aromatic hydrocarbon (PAH) complexes have become the focus of many studies. The interest in TM-PAH complexes stems from the fact that PAH molecules offer more flexibility in the size of the $\pi$ surface and the number of binding sites, as opposed to benzene molecule. One can vary the number of carbon rings by size selecting PAH molecules and, thus, can control the available binding sites for TM clusters. This controlled generation of specific size metal-organic complexes may lead to novel TM-PAH complexes with unique structural and magnetic properties. In addition, PAHs can be used to represent a finite section of graphite or a large diameter nanotube. Thus, by understanding the geometrical and electronic structure of TM-PAH complexes, one can gain insight into larger systems such as TM decorated carbon nanotube or TM clusters deposited on a graphene surface. Several studies for metal-PAH complexes have been reported previously. Dunbar[10] and Pozniak and Dunbar[42] generated several different metals reacting with one or more coronene molecules. Duncan and co-workers reported photodissociation studies for positively charged metal-coronene systems,[3,7–9,13,14,44] Nb-, Fe-, and Ca-pyrene systems,[13,44,45] and metal-corannulene complexes,[4] as well as the photoelectron spectroscopic studies (with Nakajima) for V- and Ti-coronene cluster anions.[11] Fe-PAH complexes were studied theoretically by Senapati *et al.*,[61] Wang *et al.*,[50] and Simon and Joblin.[47] Our group studied several TM-organic complexes using mass spectrometry and negative ion photoelectron spectroscopy, including benzene,[15,54,55] pyridine,[12] coronene,[23,69] pyrene,[70] and cyclooctatetraene[71] as organic ligands. Based on joint experimental and theoretical efforts, we have recently reported the geometric and electronic structure and magnetic properties of anionic and neutral TM-PAH complexes, such as $\mathrm{Co}_m(\text{coronene})_n$,[23] $\mathrm{Fe}_m(\text{coronene})_n$,[69] and $\mathrm{Fe}_m(\text{pyrene})_n$.[70]

Here, we report the spectroscopic study combined with theoretical calculations for negatively charged $\mathrm{Co}_m(\text{pyrene})_n^-$ ($m=1,2$; $n=1,2$) and their corresponding neutral complexes. Thus, we expect the current work in conjunction with our earlier work[23] on $\mathrm{Co}_m(\text{coronene})_n$ complexes to provide a more complete picture of the geometries, electronic structure, and magnetic properties of Co atoms

[a]Authors to whom correspondence should be addressed. Electronic addresses: akandalam@mcneese.edu and kbowen@jhu.edu.
[b]Present address: Department of Physics, McNeese State University, Lake Charles, LA 70605, USA.

and dimers supported on flat PAH surfaces. In addition, a comparison of the current work with analogous systems [viz., Co(benzene) and Co(coronene) systems] will act as a guide for understanding the effect of the size of the carbon network on the structural and most importantly on the magnetic properties of Co clusters when deposited on carbon nanostructures.

## II. METHODS

### A. Experimental

Negative ion photoelectron spectroscopy is governed by the energy-conserving relationship, $h\nu = EBE + EKE$, where $h\nu$ is the photon energy, EBE is the electron binding energy, and EKE is the electron kinetic energy. The laser vaporization technique was used to produce the $Co_m(pyrene)_n$ ($m = 1-2$, $n = 1-2$) cluster anions in the ion source, and the same method was used to generate metal-PAH cluster anions in our previous reports. In the source, a Nd:YAG (yttrium aluminum garnet) laser operating at 532 nm ablated a rotating, translating pyrene-coated cobalt rod. The cluster anions were cooled by helium gas from a pulsed valve ($\sim$4 atm) and then extracted into a linear time-of-flight mass spectrometer with the resolution of $\sim$600, where they were mass selected and photodetached with the third harmonic frequency (355 nm, 3.49 eV) of another Nd:YAG laser. The resulting photodetached electrons were then energy analyzed with a magnetic bottle, electron energy analyzer having a resolution of $\sim$50 meV at EKE = 1 eV. Our apparatus has been described in detail elsewhere.[15]

### B. Computational

Density functional theory (DFT) based electronic structure calculations of neutral and the negatively charged $Co_m(pyrene)_n$ complexes were carried out using the GAUSSIAN03 program.[72] BPW91, the gradient-corrected Becke's exchange[73] combined with Perdew–Wang correlation functional[74] were used in these calculations. The carbon and hydrogen atoms of pyrene were represented by the triple-$\zeta$ basis set, 6-311G**, while relativistic effective frozen-core Lanl2dz basis set was used for Co atoms. The ground state structures of both neutral and anionic $Co_m(pyrene)_n$ complexes were obtained by carrying out geometry optimization of various structural isomers without any symmetry constraints. In the geometry optimization procedure, the convergence criterion for energy was set to $10^{-9}$ hartree, while the gradient was converged to $10^{-4}$ hartree/Å. In addition, different possible spin multiplicities were also considered for each of these structural isomers to determine the preferred spin states of these complexes. In order to determine the stability of these complexes, vibrational frequency calculations were carried out for the three lowest energy structural configurations. The accuracy and reliability of our theoretical method, specifically the functional form and the basis set, have been very well established in our previous studies[23,56,69] on different metal-organic complexes. The transition energies are computed as the energy difference between the anion and neutral complexes, both calculated at the optimized geometry of anionic
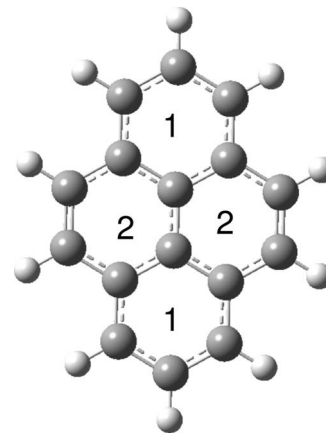


FIG. 1. Pyrene $(C_{16}H_{10})$ molecule. The two different carbon rings are identified.

complex. Note that the lowest vertical transition energy is termed as vertical detachment energy (VDE) of the complex. The electron affinity (EA) of the neutral complex is calculated as the energy difference between the anion and the neutral ground state geometries.

## III. RESULTS AND DISCUSSION

Pyrene $(C_{16}H_{10})$ is one of the smallest *ortho-* and *peri-*fused PAHs containing four benzene rings fused together (see Fig. 1). Thus, pyrene has two different types of carbon rings: one carbon ring (termed as ring-1) shares three carbon atoms with two other rings, while the other type of carbon ring (termed as ring-2) shares four carbon atoms with three other carbon rings (see Fig. 1). The TM atoms/ions have $\eta^6$-binding, $\eta^3$-binding, and $\eta^2$-binding sites available on both of these carbon rings of pyrene.

The photoelectron spectra of $Co_m(pyrene)_n^-$ ($m = 1, 2$; $n = 1, 2$) anions obtained from our experiments are shown in Fig. 2. The calculated lowest energy structures of neutral and
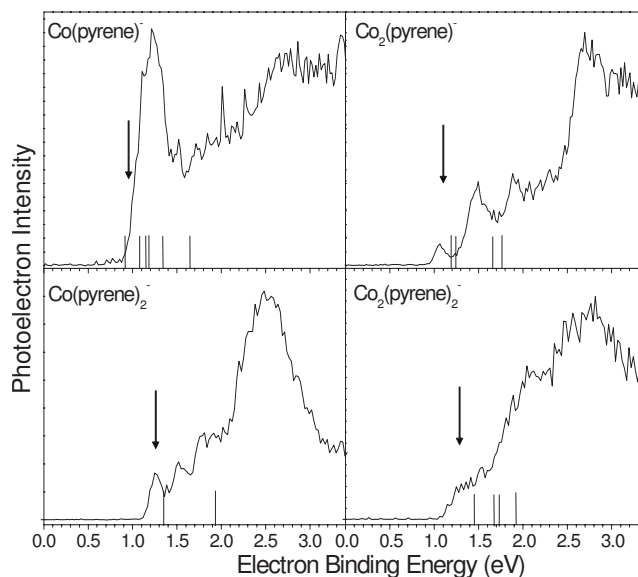


FIG. 2. The photoelectron spectra of $Co_m(pyrene)_n^-$ ($m = 1-2$, $n = 1-2$) complexes. The arrows indicate the calculated EA values, while the sticks mark the calculated photodetachment transition energies.
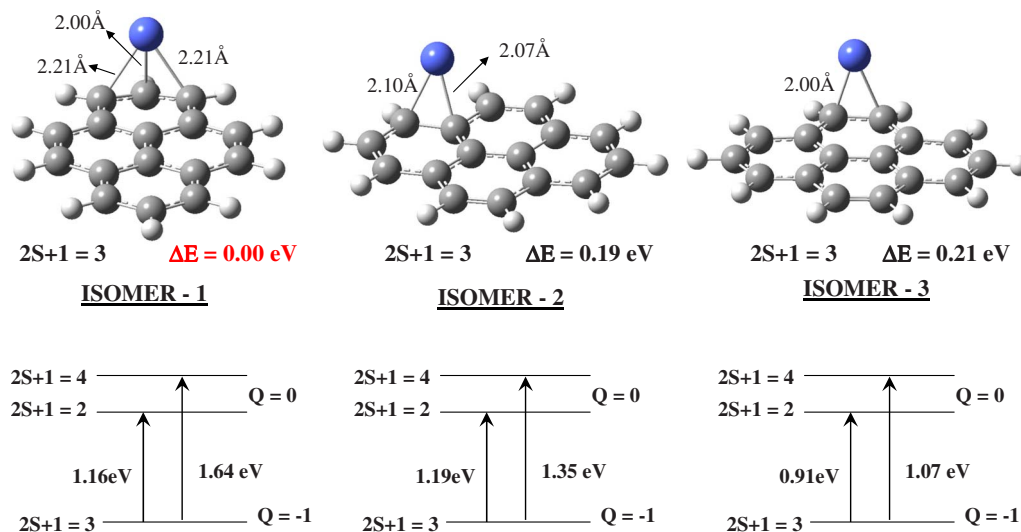
FIG. 3. (Color online) The three lowest energy isomers of the Co(pyrene)$^-$ complex along with the relative energies and their spin multiplicities. The calculated transition energies are also given.

negatively charged $Co_m(pyrene)_n$ ($m=1,2$; $n=1,2$) complexes are given in Fig. 3, 5–11, while the calculated transition energies and EAs are compared with the measured values in Table I.

## A. Co(pyrene)$^-$ and Co(pyrene)

The photoelectron spectrum of Co(pyrene)$^-$ shows a strong feature between 1.0 and 1.5 eV, followed by broad band or bands that cover its higher EBE region. The spectrum shows some similarity with that of the Co(coronene)$^-$ complex[23] in that both spectra are composed of a strong peak, followed by broad band(s), although in the spectrum of Co(pyrene)$^-$, the strong feature looks like a combination of two or more peaks since there is a shoulder before the peak which is located at 1.11 eV. The EA value of Co(pyrene) is estimated to be 0.93 eV.

According to our theoretical calculations there are three different stable isomers for the Co(pyrene)$^-$ (anionic) complex (Fig. 3). In the lowest energy isomer (Fig. 3, isomer-1), the Co atom binds to three carbon atoms ($\eta^3$) of ring-1 of pyrene molecule. The average Co–C bond length in this iso-

mer is found to be 2.14 Å. In the next two lower energy isomers, the Co atom prefers $\eta^2$-binding sites (Fig. 3, isomer-2, isomer-3). In isomer-2 ($\Delta E=0.19$ eV), the Co atom has $\eta^2$ coordination with the C–C bond of ring-1 of pyrene, while in isomer-3 ($\Delta E=0.21$ eV), the $\eta^2$-coordinated Co atom is located on the C–C bridge site of ring-2 of pyrene. All the three isomers of Co(pyrene)$^-$ complex prefer triplet ($2S+1=3$) spin state. It is noteworthy here that the Co(coronene)$^-$ complex, reported in our earlier study,[23] also prefers a triplet spin state. Since all the three isomers reported here are energetically very close and are within the uncertainty of our method, we have calculated the electron-detachment transition energies of all three isomers (Fig. 3). The calculated electron-detachment energies for the lowest energy isomer (isomer-1) are 1.16 and 1.64 eV, which correspond to transition from anion triplet to neutral doublet and neutral quartet, respectively. For isomer-2, with $\eta^2$-coordinated Co on ring-1, the calculated transition energies are 1.19 eV (triplet to doublet) and 1.35 eV (triplet to quartet), while the transition energies of isomer-3 ($\eta^2$-coordinated Co on ring-2) are calculated to be 0.91 eV

TABLE I. The experimental and calculated EA values and photodetachment energies of $Co_m(pyrene)_n$ ($m,n=1,2$) complexes. The vibrational zero-point corrections are not included in the predicted EA values.

| | EA (eV) | | VDE (eV) | | Transitions to exited states of neutral (eV) | | Spin multiplicity ($2S+1$) |
|---|---|---|---|---|---|---|---|
| | Expt. | Theor. | Expt. | Theor. | Expt. | Theor. | |
| Co(pyrene) | 0.93 | 0.96 | 1.11 | Isomer-1: 1.16 | 1.22 | Isomer-2: 1.35 | 2 |
| | | | | Isomer-2: 1.19 | | Isomer-1: 1.64 | |
| | | | | Isomer-3: 0.91 | | Isomer-3: 1.07 | |
| $Co_2(pyrene)$ | 0.95 | 1.10 | 1.06 | Isomer-2: 1.19 | 1.49 | Isomer-2: 1.65 | 5 |
| | | | | Isomer-1: 1.23 | 1.89 | Isomer-1: 1.76 | |
| | | | | | 2.70 | | |
| $Co(pyrene)_2$ | 1.12 | 1.27 | 1.25 | 1.35 | 1.51 | 1.92 | 2 |
| | | | | | 1.80 | 2.10 | |
| $Co_2(pyrene)_2$ | 1.11 | 1.29 | 1.35 | Isomer-1: 1.45 | 2.10 | Isomer-1: 1.92 | 1 |
| | | | | Isomer-2: 1.68 | 2.75 | | |
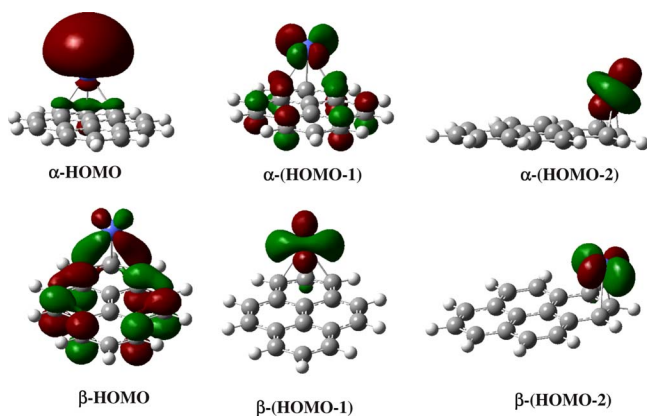
FIG. 4. (Color online) The frontier MOs. of isomer-1 of $[Co(pyrene)]^-$ complex. The first row corresponds to the $\alpha$ MOs, while the second row corresponds to $\beta$ MOs.

(triplet to doublet) and 1.07 eV (triplet to quartet). The calculated transitions for all the three isomers are in good agreement with the measured EBE values of 1.1 and 1.22 eV (see Table I). Therefore, in the $Co(pyrene)^-$ spectrum shown in Fig. 1, the broadening of the first peak (from 1.0 to 1.5 eV) is most likely due to the overlap of the transitions from all the three lowest energy isomers. Thus, we cannot rule out the possibility of any of the three isomers in the cluster beam and thus in the observed photodetachment transitions. The similarities in the binding of Co atom to pyrene and coronene are further manifested in the nature of their frontier molecular orbitals (MOs). In all the three isomers of $Co(pyrene)^-$, similar to that seen in the $Co(coronene)^-$, the frontier MOs are dominated by those with antibonding or nonbonding character (Fig. 4). The exceptions are the $\beta$-HOMO (HOMO denotes highest occupied molecular orbital) of isomer-1 and isomer-2. For example, in isomer-1, the $\beta$-HOMO is a bonding orbital having bonding characteristics between $d_{yz}$ of Co and $\pi$ orbitals of pyrene, while the remaining frontier $\beta$-MOs are nonbonding in nature (see Fig. 4).

The neutral Co(pyrene) complex, our calculations predict two stable, isoenergetic structures, one in which the Co atom has $\eta^3$ coordination (Fig. 5, isomer-1) and other with a
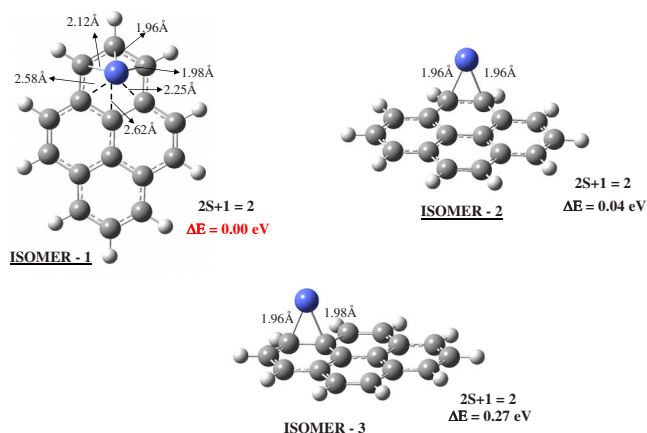


FIG. 5. (Color online) The three lowest energy structures of the Co(pyrene) complex. The relative energies and their spin multiplicities $(2S+1)$ are also given.

$\eta^2$-coordinated Co atom located on ring-2 (Fig. 5, isomer-2). These isomers are energetically degenerate with an energy difference of just 0.04 eV. The lowest energy isomer of neutral Co(pyrene) is similar to its anion counterpart, with the Co atom binding to ring-1 of the pyrene molecule with $\eta^3$ coordination (Fig. 5, isomer-1). However, unlike in anionic $Co(pyrene)^-$, in the case of the neutral cluster, the binding of the Co atom to pyrene resulted in puckering of the planar pyrene molecule. The average bond length of Co–C in this neutral cluster is 2.02 Å. A third structural isomer (Fig. 5, isomer-3) in which the Co atom is bound to the C–C bond on ring-1 ($\eta^2$) is found to be 0.27 eV higher in energy. Note that the energy ordering of the two $\eta^2$-isomers is reversed when compared with the $Co(pyrene)^-$ anionic isomers. Overall, in neutral as well as in anionic Co(pyrene) complexes, the Co atom prefers the $\eta^2$-binding site over $\eta^6$-binding site. We are not aware of any earlier studies on the Co(pyrene) complex. Interestingly, in our earlier study[23] on neutral Co(coronene), we observed a strong competition ($\Delta E = 0.02$ eV) between the $\eta^6$- and $\eta^2$-binding sites in stabilization of the complex. In an earlier theoretical study,[47] it was reported that for the ground state geometry of the neutral Fe(pyrene) complex, the Fe atom preferred to bind over ring-2 of the pyrene with $\eta^2$ coordination.

The calculated EA for the Co(pyrene) complex is 0.96 eV, which is in excellent agreement with the measured value of $0.93 \pm 0.10$ eV. The neutral Co(pyrene) complex prefers a doublet $(2S+1=2)$ spin state, which corresponds to a spin magnetic moment of $1\mu_B$. It is to be noted here that free Co atom $(2S+1=4)$ has a spin magnetic moment of $3\mu_B$. In a recent theoretical study[65] on $Co_n(benzene)_m$ complexes, the Co(benzene) complex was also reported to have a doublet spin state. Thus, comparing the earlier works[23,62] of Co(coronene) $[(2S+1=2)]$ and Co(benzene) with the current results, we note that the spin magnetic moment of Co atom becomes significantly reduced from its atomic magnetic moment when interacted with aromatic and polycyclic aromatic hydrocarbons. In addition, the size of the carbon network appears to have no effect on the reduced magnetic moment of the Co atom.

### B. Co$_2$(pyrene)$^-$ and Co$_2$(pyrene)

Four features are observed in the spectrum of $Co_2(pyrene)^-$ which are located at 1.06, 1.49, 1.89, and 2.70 eV. The EA of neutral $Co_2(pyrene)$ is estimated to be 0.95 eV. We observe that the spectra of all of the previously reported $Co_2(organic)^-$ complexes, including benzene,[15] pyridine,[12] and coronene,[23] show three small peaks which have an almost identical pattern to the spectrum of $Co^-$ atom[15] plus a strong peak at higher binding energy side. Here in the spectrum of $Co_2(pyrene)^-$, a similar pattern was observed implying that the $Co_2(pyrene)^-$ can be set in the same category as the other $Co_2(organic)^-$ systems and that all of these systems are expected to share similar geometrical structure. As reported in our previous work,[23] in the ground state $Co_2(coronene)^-$ complex, the Co atoms dimerize and bind to the outer ring with the dimer axis perpendicular to the coronene. The electron density was found to be mostly
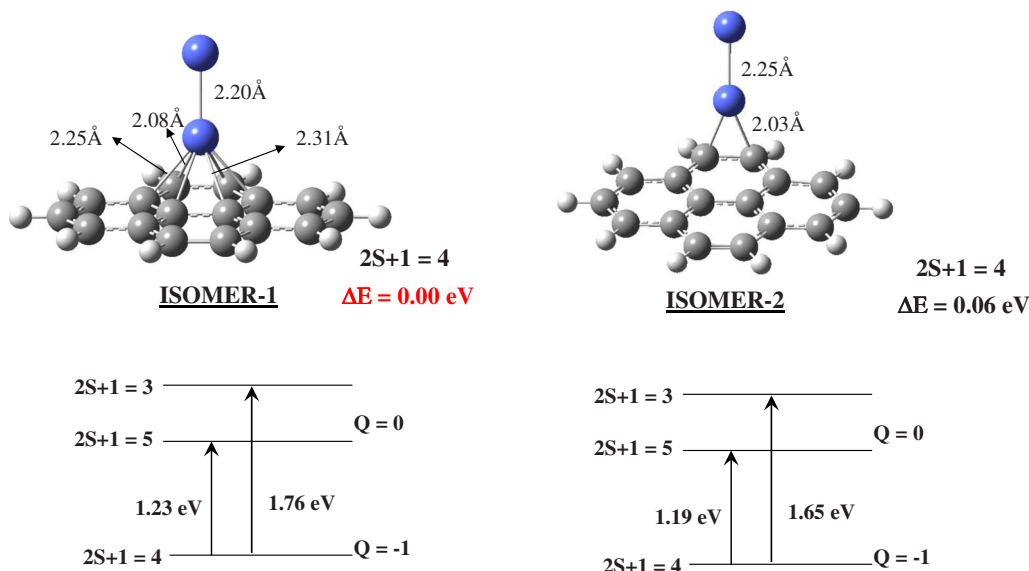
FIG. 6. (Color online) The two most stable geometries of the $Co_2(pyrene)^-$ complex, along with their spin multiplicities and relative energies. The vertical transition energies calculated for both the isomers are also given.

localized on the distal Co atom, thus explaining the observation of the characteristic signature of $Co^-$ rather than that of $Co_2^-$ in the $Co_2(coronene)^-$ spectrum. Therefore, based on the similarities in photoelectron spectra, the structure of $Co_2(pyrene)^-$ is also expected to have the cobalt dimer perpendicular to the pyrene ring.

Our calculations show that there are two stable and energetically degenerate ($\Delta E=0.06$ eV) isomers for $Co_2(pyrene)^-$ (Fig. 6). As expected, in both of these isomers, the Co atoms form dimers, with the dimer bond axis almost perpendicular to ring-2 of the pyrene molecule. The notable difference between these two isomers is in the coordination of the proximal Co atom: while it is $\eta^6$ coordination in isomer-1, in isomer-2 it is $\eta^2$ coordination. Interestingly, isomer-1 is similar to the previously reported[69] ground state structure of $Fe_2(coronene)^-$, while isomer-2 is similar to the previously reported[23] ground state structure of $Co_2(coronene)^-$. The Co–Co bond lengths in isomer-2 of $Co_2(pyrene)^-$ in the ground state geometry[23] of $Co_2(coronene)^-$ and in the $Co_2$ dimer are 2.25, 2.26, and 2.15 Å, respectively. Thus, even though the Co–Co bond weakens due to its interaction with the organic ligands, the size of the PAH molecule has negligible effect on the Co–Co

bond length. In addition, $Co_2(pyrene)^-$ prefers a quartet ($^4A'$) spin multiplicity, which is again the same as that of the $Co_2(coronene)^-$ complex. The other higher energy isomers of $Co_2(pyrene)^-$ are given in Fig. 7. The common structural feature among these isomers is that *both* the cobalt atoms are directly bound to the pyrene molecule and *always* have the $\eta^2$ coordination. None of the structures with $\eta^6$ coordination for both the Co atoms are found to be near a minimum. These higher energy isomers are also identical with previously reported[23] higher energy isomers of $Co_2(coronene)^-$. The charge analysis of isomer-2 of $Co_2(pyrene)^-$ revealed that the extra electron was mostly localized on the distal cobalt atom, with a Mulliken charge of $-0.42e$, while the proximal Co atom has a Mulliken charge of $+0.04e$ only. These unequal charges on the Co atoms and a greater charge distribution on distal Co atom are likely responsible for the $Co^-$ characteristics observed in the photoelectron spectrum of $Co_2(pyrene)^-$. It is worth mentioning here that an identical charge distribution picture was observed in $Co_2(coronene)^-$ complex.

As mentioned above, the ground state spin multiplicity of both of the isomers of $Co_2(pyrene)^-$ is quartet ($2S+1 =4$). The calculated electron-detachment transition energies



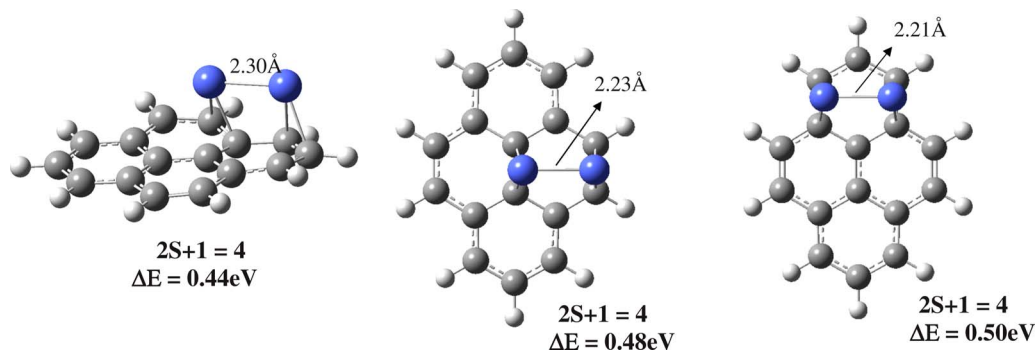FIG. 7. (Color online) The higher energy isomers of the $Co_2(pyrene)$-complex. The relative energies (eV) compared to the lowest energy isomer (isomer-1, Fig. 5) and the spin multiplicities are also shown.
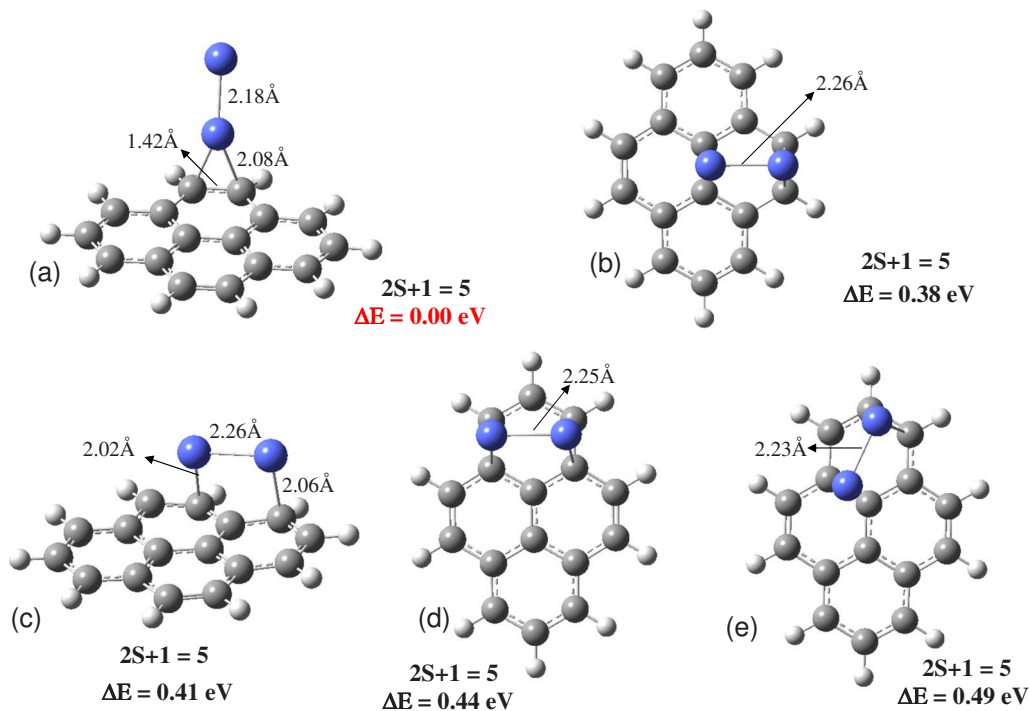
FIG. 8. (Color online) The ground state and the higher energy isomers of the neutral $Co_2$(pyrene) complex. The relative energies and the spin multiplicities are also shown.

are 1.23 eV (quartet to quintet) and 1.76 eV (quartet to triplet) for isomer-1, and 1.19 eV (quartet to quintet) and 1.65 eV (quartet to triplet) for isomer-2. The transition energies from both of these isomers are in good agreement with the experimentally measured values of 1.06 and 1.49 eV, indicating the possibility of both the isomers contributing to the observed peaks in the experiment. The electronic structure analysis of isomer-2 shows that the frontier MOs have antibonding character between the metal atoms. For example, the first electron detachment, corresponding to VDE $=1.19$ eV is from a $d_{x^2-y^2}$ antibonding $\beta$-MO between the metal atoms. Similarly, the first transition to neutral triplet (EBE$=1.65$ eV) in isomer-2 is from a $d_{x^2-y^2}$ antibonding $\alpha$-MO. This electronic structure picture is identical to that seen in the previously reported $Co_2$(coronene)$^-$ complex. Thus, the similarities in the photoelectron spectra of $Co_2$(pyrene)$^-$ and $Co_2$(coronene)$^-$ may be due to the preponderance of isomer-2 over isomer-1 in the cluster beam.

If we compare the peak positions of $Co_2$(pyrene)$^-$ with those of $Co^-$ in their respective photoelectron spectra (Table 3 in Ref. 23), we find that the peaks of $Co_2$(pyrene)$^-$ have shifted to higher EBEs by about ~0.3 eV as compared to $Co^-$ spectrum. However, this peak shift is smaller than those seen in $Co_2$(benzene)$^-$ (~0.7 eV) (Ref. 15) and $Co_2$(coronene)$^-$ (~0.55 eV).[23] Since the complexity of the carbon network in pyrene is intermediate between benzene and coronene, it is a surprise not to observe a similar intermediate stabilization effect. This is probably due to a stronger interaction between the metal and benzene as compared to the extended carbon network. It is also reasonable to see the coronene behaving as a stronger stabilizer than pyrene because of its bigger $\pi$ surface.

In the ground state geometry of neutral $Co_2$(pyrene)

complex, the cobalt dimer is bound to the $\eta^2$ site on ring-2 of the pyrene, with its bond axis perpendicular to the pyrene molecule [Fig. 8(a)]. The Co–Co bond length (2.18 Å) in this isomer is comparable to the corresponding bond lengths in $Co_2$ dimer (2.15 Å) and $Co_2$(coronene)$^-$ (2.21 Å). The ground state $Co_2$(pyrene) has a spin multiplicity of quintet ($2S+1=5$). The calculated EA is 1.10 eV, which is in good agreement with the experimental value of 0.95 eV. The ground state structure of the neutral complex is identical to isomer-2 (see Fig. 6) of $Co_2$(pyrene)$^-$. Interestingly, the isomer with Co atoms/dimer occupying the $\eta^6$-binding site, the lowest energy structure of $Co_2$(pyrene)$^-$, is not even a local minimum in the case of neutral complex. In fact, when $Co_2$ dimer was placed at the $\eta^6$-binding site, during the geometry optimization process, the $Co_2$ moved away from the center of the ring onto the C–C bridge site, thus attaining $\eta^2$ coordination. The ground state geometries of $Co_2$(pyrene) and our earlier reported[23] $Co_2$(coronene) have definite structural similarities: in both cases, the Co atoms dimerize and only one Co atom directly binds to the C–C edge ($\eta^2$ site), with the dimer bond axis perpendicular to the corresponding PAH molecule. Furthermore, the higher energy isomers of $Co_2$(pyrene) shown in Fig. 8 are not only the same as their anion counterparts but are also similar to the higher energy isomers[23] of neutral $Co_2$(coronene) complexes. Thus, the similarities in the lowest energy and higher energy structures, Co–Co bond lengths of $Co_2$(coronene) and $Co_2$(pyrene) indicate that the size of the carbon (PAH) network has a negligible effect on the geometrical structure of $Co_m$(PAH) systems.

As mentioned above, the $Co_2$(pyrene) neutral complex prefers quintet ($2S+1=5$) as its ground state spin multiplicity, and this gives it a spin magnetic moment of $4\mu_B$. It is
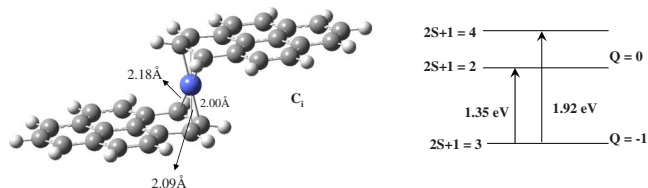
FIG. 9. (Color online) The ground state structure of the $Co(pyrene)_2^-$ complex. The spin multiplicity and the calculated vertical transition energies are also given.

interesting to note here that, while bare Co atom has a spin magnetic moment of $3\mu_B$, the bare $Co_2$ dimer has a spin magnetic moment of only $4\mu_B$, which corresponds to $2\mu_B$/atom. Therefore, one has to be careful while interpreting the effect of the pyrene molecule on the spin magnetic moment of metal atom/cluster. It is tempting to compare the spin magnetic moment per Co atom in $Co_2(pyrene)$, which is $2\mu_B$/atom, with Co atom's spin moment and conclude that the spin magnetic moment of Co atom in $Co_2(pyrene)$ complex is reduced from its atomic value of $3\mu_B$. However, when we consider a different scenario, in which the $Co_2$ *dimer*, taken as one unit is interacting with the pyrene molecule, then it can be seen that pyrene molecule has absolutely no effect on the spin magnetic moment of $Co_2$ dimer. We think that the latter interpretation is more appropriate for the current situation since in the ground state geometry of $Co_2(pyrene)$, a $Co_2$ dimer interacts with the pyrene molecule. In $Co_2(pyrene)$, the Co atoms are ferromagnetically coupled with a local spin moment of $1.78\mu_B$ on distal Co and $2.33\mu_B$ on frontal Co atom, while pyrene molecule carries a small negative moment of $-0.11\mu_B$. In our previous study[23] of $Co_2(coronene)$ complex, we reported an identical scenario of ferromagnetic coupling between Co atoms with the spin magnetic moment of the $Co_2(coronene)$ being $4\mu_B$. Thus, we generalize that two Co atoms, when supported on *any* PAH template, not only dimerize but also prefer to maintain a ferromagnetic coupling between them. Furthermore, the net spin magnetic moment of the dimer ($4\mu_B$) is not affected significantly by the PAH molecule.

## C. $Co(pyrene)_2^-$ and $Co(pyrene)_2$

The spectrum of $Co(pyrene)_2^-$ shows three small peaks followed by a much stronger peak at high EBE. The small peaks are centered at 1.25, 1.51, and 1.80 eV, and the big peak is located at $\sim 2.5$ eV. The EA of the neutral $Co(pyrene)_2$ is estimated from the spectrum to be 1.12 eV, while the VDE of $Co(pyrene)_2^-$ is measured as 1.25 eV. As in $Co_2(pyrene)^-$, the first three peaks are reminiscent of those in the spectrum of atomic $Co^-$, although the spacing between the peaks are much closer.

Theoretical calculations show that $Co(pyrene)_2^-$ is a staggered sandwich (steplike) structure (Fig. 9) with the Co atom sandwiched at the edge of the pyrene molecules and has $\eta^3$-coordinated bonding. The spin multiplicity of $Co(pyrene)_2^-$ is calculated to be a triplet ($2S+1=3$). The $Co(pyrene)_2^-$ complex is similar to our recently reported[69] ground state geometry of $Fe(coronene)_2^-$ complex. However, unlike in $Fe(coronene)_2^-$, there is no overlap between the

carbon rings of the two pyrene molecules. The vertical transition energies of $Co(pyrene)_2^-$ are 1.35 eV (anion triplet to neutral doublet) and 1.92 eV (anion triplet to neutral quartet). The calculated transition energies are in good agreement with the measured values of 1.25 and 1.51 eV. In addition, the higher energy peak (EBE=1.80 eV) is due to an electron detachment from a $\beta$-MO, which corresponds to calculated transition energy of 2.10 eV. The next set of higher transition energies are calculated to be 2.30 and 2.60 eV from $\alpha$-MOs and 2.70 eV from $\beta$-MO. These closely spaced transition energies contribute to the observed broad peak centered at $\sim 2.5$ eV (Fig. 1).

For neutral $Co(pyrene)_2$ complex, calculations show that there are four stable and energetically close ($\Delta E_{max}$ =0.11 eV) sandwich structures (Fig. 10). Of the four sandwich structures, three of them are staggered or steplike [in Figs. 10(a), 10(b), and 10(d)], while one structure is a normal (eclipsed) sandwich [Fig. 10(c)]. All these isomers prefer a doublet spin multiplicity ($2S+1=2$). The calculated EA of 1.27 eV is in good agreement with the experimental value of 1.12 eV. An examination of the most stable neutral isomers reveals that in the first isomer [Fig. 10(a)], the pyrene molecules are not parallel to each other and the Co–C distances are different, while the second isomer [Fig. 10(b)] is more symmetric ($C_{2h}$) with both the pyrene molecules parallel to each other. The next energy isomer ($\Delta E=0.11$ eV) is a normal sandwich structure ($C_s$), with the Co atom binding at the edges of the pyrene molecules ($\eta^2$). Since the interaction of the Co and pyrene is confined to one edge of the pyrene molecules, the opposite ends of the pyrene molecule are bent away from each other, thus opening up the normal sandwich structure. In the other higher energy ($\Delta E=0.11$ eV) staggered sandwich [Fig. 10(d)], the Co atom has $\eta^6$ coordination with one pyrene and $\eta^2$ coordination with the other pyrene molecule. The first two staggered sandwich structures [Figs. 10(a) and 10(b)] are similar to our recently reported[69] stable isomers of $Fe(coronene)_2$ complex.

Since the neutral $Co(pyrene)_2$ complex has a doublet spin multiplicity, the Co atom has spin magnetic moment of $1\mu_B$. Thus, following the trend, first seen in the case of $Co(coronene)$ and then again in $Co(benzene)$ and $Co(pyrene)$ complexes, the magnetic moment of Co atom gets significantly reduced from its atomic spin magnetic moment when it is supported on an organic template.

## D. $Co_2(pyrene)_2^-$ and $Co_2(pyrene)_2$

While there is less structure in the spectrum of $Co_2(pyrene)_2^-$, the signal can still be identified as the combination of at least three bands. The threshold of the spectrum (EBE=1.11 eV) is estimated as the EA of neutral $Co_2(pyrene)_2$. The VDE is taken as the center position of the first discernible band, which is around 1.35 eV. Other transitions to the excited states of the neutral occur at around 2.10 and 2.75 eV.

Our calculations show that there are two very similar stable structures for $Co_2(pyrene)_2^-$ complex (Fig. 11). Both these isomers are staggered sandwich structures, with Co atoms sandwiched between the pyrene molecules. Note that in
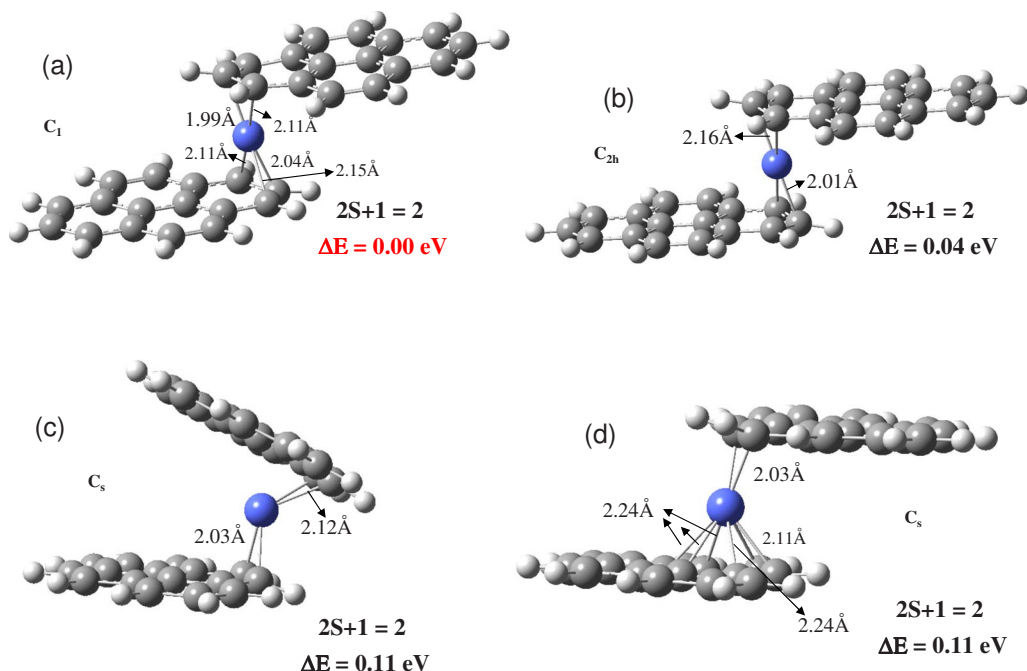
FIG. 10. (Color online) The ground state and higher energy isomers of the neutral Co(pyrene)$_2$ complex.

the lowest energy structure (Fig. 11, isomer-1), the pyrene molecules are linked by a weak Co dimer with Co–Co bond length of 2.43 Å, while in the higher energy isomer ($\Delta E$ = 0.16 eV) there is no Co–Co bond present (Co–Co: 2.78 Å). Notwithstanding these minor differences in both these isomers, the Co atoms bind only to the edge sites ($\eta^2$ site) of the pyrene molecule, with no overlap between the carbon rings

of the pyrene. In fact, when the Co atoms are placed at the center ($\eta^6$) of the carbon rings with overlap between the carbon rings of pyrene molecules, the rings along with the Co atoms moved away and finally formed nonoverlapping, staggered sandwich structures with $\eta^2$-coordinated Co atoms during geometry optimization. There is another higher energy structure ($\Delta E \approx 0.37$ eV), in which the Co atoms are
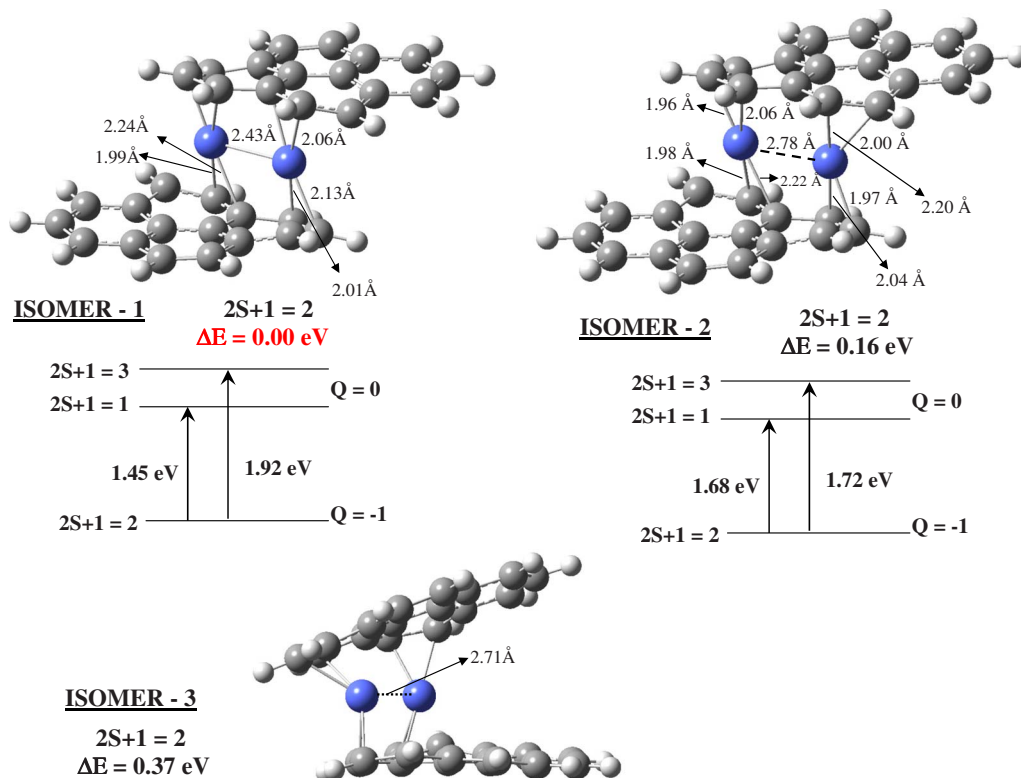


FIG. 11. (Color online) The ground state and the higher energy isomers of the Co$_2$(pyrene)$_2^-$ complex. The spin multiplicity and the calculated vertical transition energies are also given for lowest two isomers.
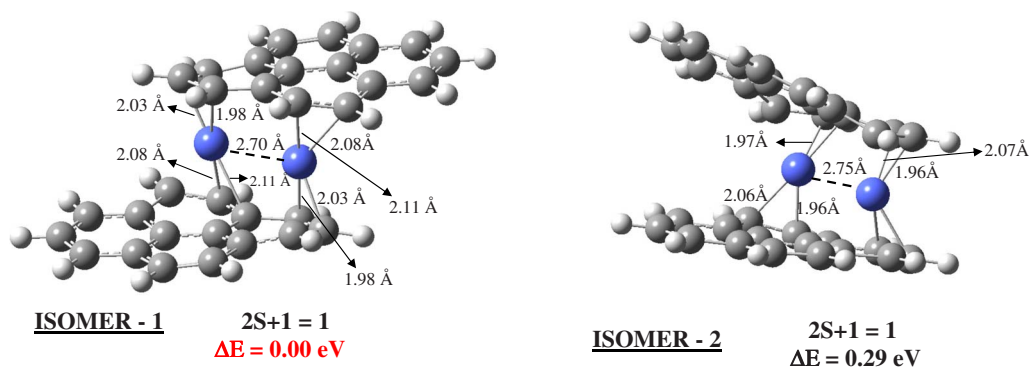
FIG. 12. (Color online) The ground state and higher energy isomers of the neutral $Co_2(pyrene)_2$ complex.

sandwiched between the two pyrene molecules (Fig. 11, isomer-3). However, in this structure the pyrene molecules form a normal/regular sandwich, with Co atoms again preferring to have $\eta^2$ binding on the edges of the pyrene molecules. All three of these isomers are in doublet $(2S+1=2)$ spin states. These sandwich structures are similar to the earlier reported[69] geometries of $Fe_2(coronene)_2^-$ complex. Another staggered sandwich structure, in which the Co dimer has its bond axis perpendicular to the pyrene molecules, is found to be 1.85 eV higher in energy (not shown here). This isomer has a spin multiplicity of 4.

For the lowest energy isomer (isomer-1), the calculated lowest two transition energies are 1.45 and 1.92 eV, corresponding to transition from anion doublet to neutral singlet and neutral triplet states, respectively. In the higher energy isomer (isomer-2), the transition energies are calculated to be 1.68 eV (double to singlet) and 1.72 eV (doublet to triplet). Comparing these transition energies with the measured values, it appears that the lowest energy isomer contributes to the first (1.35 eV) and second (2.10 eV) peaks of the photoelectron spectrum. However, the contribution from the higher energy isomer to the photoelectron spectrum cannot be completely ruled out as its transition energies do match with other small unidentified peaks. In fact, the broad bands in the photoelectron spectrum indicate the possibility of multiple structural isomers being present in the cluster beam, thus contributing to the photoelectron spectrum.

Two stable sandwich structures are predicted as the lowest energy isomers for neutral $Co_2(pyrene)_2$ complex, with both of them preferring a singlet $(2S+1=1)$ spin multiplicity (see Fig. 12). The staggered sandwich structure is (isomer-1) is 0.29 eV more stable than the normal/partially eclipsed sandwich structure (isomer-2). It was reported[62] earlier that $Co_2(benzene)_2$ cluster forms a normal sandwich structure, with both the Co atoms sandwiched between the benzene molecules. Similar staggered and eclipsed sandwich structures were reported earlier[69] for $Fe_2(coronene)_2$ complex. Based on these similarities, it is expected that $Co_2(coronene)_2$ would be either a staggered or an eclipsed sandwich structure. One can further generalize this to other TM and PAH molecules, and suggest that, in general, the neutral and charged $TM_m(PAH)_n$ complexes, for $n=2$ and $m>1$, prefer to form stable sandwich structures. The EA of $Co_2(pyrene)_2$ complex is calculated to be 1.29 eV, which is in good agreement with the estimated value of 1.11 eV. In

the lowest energy isomer (isomer-1), the singlet spin state is energetically degenerate with the high-spin triplet state ($\Delta E =0.06$ eV). Interestingly, a similar scenario in which the singlet and triplet states compete in the stabilization of TM (organic) complexes was observed in the previously reported study[62] of $Co_2(benzene)_2$ clusters. However, in the case of $Co_2(benzene)_2$, it was the triplet which is lower in energy ($\Delta E=0.02$ eV) than the singlet state. Since the two spin states are energetically degenerate, $Co_2(pyrene)_2$ can have either of these spins. If we consider the high-spin state (triplet), we get a spin magnetic moment of $2\mu_B$ for $Co_2(pyrene)_2$ complex, thus $1\mu_B/Co$ atom. If we compare this spin moment with those of bare $Co_2$ cluster and $Co_2(pyrene)$ complex, it becomes evident that the second pyrene molecule quenches the spin magnetic moment of metal cluster to its minimum value.

## IV. SUMMARY AND CONCLUSIONS

Negatively charged $Co_m(pyrene)_n$ $(m=1-2, n=1-2)$ complexes were generated in a laser vaporization source. These complexes were studied by anion photoelectron spectroscopy and DFT based theoretical calculations. By this synergetic approach, we have identified the ground state geometries and studied the electronic structure and magnetic properties of both neutral and anionic $Co_m(pyrene)_n$ complexes.

From our current work it was clearly discernible that the $Co_m(pyrene)_n$ complexes form sandwich structures (for $n =2$). While our recent study[69] on $Fe_m(coronene)_n$ complexes has confirmed the existence of sandwich or sandwichlike structures for TM-coronene complexes, the current work extends this scenario to TM-pyrene complexes and provides a conclusive evidence to the existence of sandwich structures in $TM_m(PAH)_n$ complexes, at least for $n=2$. Furthermore, by comparing the current system with analogous systems, such as $Co_m(benzene)_2$ and $Fe_m(coronene)_2$, it can be suggested that the size of the organic molecule has negligible effect on the structures of Co(organic) complexes and these complexes form either normal or staggered sandwich structures. However, it is anticipated that introduction of a third pyrene molecule will more likely lead to energetically competitive "rice-ball" structures, where the metal atoms form a core and the organic molecules act as a shell to the metallic core.

Most notably, the absence of a multilayered sandwich structure ($|\cdot|\cdot$), in which the pyrene and Co atoms are placed alternatively in both neutral and anionic $Co_2(pyrene)_2$ complexes, reinforces our conclusion that TM atoms, in general, when deposited on carbon $\pi$ surfaces would aggregate together and form clusters. The aggregation of metal atoms on the carbon $\pi$ surface is expected to have important implications on the magnetic of the metal clusters. In the cases of $Co_2(pyrene)_n$ ($n=1,2$) complexes, the spin magnetic moment of $Co_2$ dimer is not affected significantly, even though singlet and triplet states in $Co_2(pyrene)_2$ are competitive. However, the spin magnetic moment of Co atom in Co(pyrene) and Co(pyrene)$_2$ was quenched to its minimum possible value. This trend (i.e., quenching of spin magnetic moment as compared to its *atomic* value) is in agreement with the earlier reported studies on $Co_n-(C_6D_6)_m$ clusters,[24] Co(pyridine),[12] and Co(coronene) (Ref. 23) complexes. In a recent theoretical study[62] on $Co_n(benzene)_m$ clusters, it was reported that Co atoms preferred ferromagnetic coupling in small clusters up to $Co_3(benzene)_4$, and antiferromagnetic/ferrimagnetic coupling was seen only in $Co_4(benzene)_4$ cluster. Therefore, it would be interesting to further extend the systems under current investigation to larger sizes and explore the possibility of the presence of rice-ball structures and the onset of antiferromagnetic ordering. Experimental and theoretical investigations in this direction are in progress.

## ACKNOWLEDGMENTS

[1] I. M. L. Billas, A. Chătelain, and W. A. de Heer, Science **265**, 1682 (1994).
[2] P. Weis, P. R. Kemper, and M. T. Bowers, J. Phys. Chem. A **101**, 8207 (1997).
[3] T. M. Ayers, B. C. Westlake, and M. A. Duncan, J. Phys. Chem. A **108**, 9805 (2004).
[4] T. M. Ayers, B. C. Westlake, D. V. Preda, L. T. Scott, and M. A. Duncan, Organometallics **24**, 4573 (2005).
[5] Y. Basir and S. L. Anderson, Chem. Phys. Lett. **243**, 45 (1995).
[6] W. Branz, I. M. L. Billas, N. Malinowski, F. Tast, M. Heinebrodt, and T. P. Martin, J. Chem. Phys. **109**, 3425 (1998).
[7] J. W. Buchanan, G. A. Grieves, N. D. Flynn, and M. A. Duncan, Int. J. Mass. Spectrom. **185–187**, 617 (1999).
[8] J. W. Buchanan, G. A. Grieves, J. E. Reddic, and M. A. Duncan, Int. J. Mass. Spectrom. **182/183**, 323 (1999).
[9] J. W. Buchanan, J. E. Reddic, G. A. Grieves, and M. A. Duncan, J. Phys. Chem. A **102**, 6390 (1998).
[10] R. C. Dunbar, J. Phys. Chem. A **106**, 9809 (2002).
[11] M. A. Duncan, A. M. Knight, Y. Negishi, S. Nagao, K. Judai, A. Nakajima, and K. Kaya, J. Phys. Chem. A **105**, 10093 (2001).
[12] B. D. Edmonds, A. K. Kandalam, S. N. Khanna, X. Li, A. Grubisic, I. Khanna, and K. H. Bowen, J. Chem. Phys. **124**, 074316 (2006).
[13] N. R. Foster, J. W. Buchanan, N. D. Flynn, and M. A. Duncan, Chem. Phys. Lett. **341**, 476 (2001).
[14] N. R. Foster, G. A. Grieves, J. W. Buchanan, N. D. Flynn, and M. A. Duncan, J. Phys. Chem. A **104**, 11055 (2000).
[15] M. Gerhards, O. C. Thomas, J. M. Nilles, W.-J. Zheng, and K. H. Bowen, J. Chem. Phys. **116**, 10247 (2002).
[16] G. A. Grievesa, J. W. Buchanana, J. E. Reddic, and M. A. Duncan, Int. J. Mass. Spectrom. **204**, 223 (2001).
[17] M. Hirano, K. Judai, A. Nakajima, and K. Kaya, J. Phys. Chem. A **101**, 4893 (1997).
[18] K. Hoshino, T. Kurikawa, H. Takeda, A. Nakajima, and K. Kaya, J. Phys. Chem. **99**, 3053 (1995).
[19] N. Hosoya, R. Takegami, J.-i. Suzumura, K. Yada, K. Koyasu, K. Miyajima, M. Mitsui, M. B. Knickelbein, S. Yabushita, and A. Nakajima, J. Phys. Chem. A **109**, 9 (2005).
[20] T. D. Jaeger and M. A. Duncan, J. Phys. Chem. A **108**, 11296 (2004).
[21] T. D. Jaeger and M. A. Duncan, Int. J. Mass. Spectrom. **241**, 165 (2005).
[22] K. Judai, M. Hirano, H. Kawamata, S. Yabushita, A. Nakajima, and K. Kaya, Chem. Phys. Lett. **270**, 23 (1997).
[23] A. K. Kandalam, B. Kiran, P. Jena, X. Li, A. Grubisic, and K. H. Bowen, J. Chem. Phys. **126**, 084306 (2007).
[24] M. B. Knickelbein, J. Chem. Phys. **125**, 044308 (2006).
[25] T. Kurikawa, S. Nagao, K. Miyajima, A. Nakajima, and K. Kaya, J. Phys. Chem. A **102**, 1743 (1998).
[26] T. Kurikawa, Y. Negishi, F. Hayakawa, S. Nagao, K. Miyajima, A. Nakajima, and K. Kaya, J. Am. Chem. Soc. **120**, 11766 (1998).
[27] T. Kurikawa, Y. Negishi, F. Hayakawa, S. Nagao, K. Miyajima, A. Nakajima, and K. Kaya, Eur. Phys. J. D **9**, 283 (1999).
[28] T. Kurikawa, H. Takeda, M. Hirano, K. Judai, T. Arita, S. Nagao, A. Nakajima, and K. Kaya, Organometallics **18**, 1430 (1999).
[29] T. Kurikawa, H. Takeda, A. Nakajima, and K. Kaya, Z. Phys. D: At., Mol. Clusters **40**, 65 (1997).
[30] P. Marty, P. d. Parseval, A. Klotz, B. Chaudret, G. Serra, and P. Boissel, Chem. Phys. Lett. **256**, 669 (1996).
[31] P. Marty, P. d. Parseval, A. Klotz, G. Serra, and P. Boissel, Astron. Astrophys. **316**, 270 (1996).
[32] K. Miyajima, M. B. Knickelbein, and A. Nakajima, J. Phys. Chem. A **112**, 366 (2008).
[33] K. Miyajima, M. B. Knickelbein, and A. Nakajima, Eur. Phys. J. D **34**, 177 (2005).
[34] K. Miyajima, M. B. Knickelbein, and A. Nakajima, Polyhedron **24**, 2341 (2005).
[35] K. Miyajima, T. Kurikawa, M. Hashimoto, A. Nakajima, and K. Kaya, Chem. Phys. Lett. **306**, 256 (1999).
[36] K. Miyajima, S. Yabushita, M. B. Knickelbein, and A. Nakajima, J. Am. Chem. Soc. **129**, 8473 (2007).
[37] S. Nagao, A. Kato, A. Nakajima, and K. Kaya, J. Am. Chem. Soc. **122**, 4221 (2000).
[38] S. Nagao, T. Kurikawa, K. Miyajima, A. Nakajima, and K. Kaya, J. Phys. Chem. A **102**, 4495 (1998).
[39] S. Nagao, Y. Negishi, A. Kato, Y. Nakamura, and A. Nakajima, J. Phys. Chem. A **103**, 8909 (1999).
[40] A. Nakajima and K. Kaya, J. Phys. Chem. A **104**, 176 (2000).
[41] A. Nakajima, S. Nagao, H. Takeda, T. Kurikawa, and K. Kaya, J. Chem. Phys. **107**, 6491 (1997).
[42] B. P. Pozniak and R. C. Dunbar, J. Am. Chem. Soc. **119**, 10439 (1997).
[43] J. E. Reddic, J. C. Robinson, and M. A. Duncan, Chem. Phys. Lett. **279**, 203 (1997).
[44] A. C. Scott, J. W. Buchanan, N. D. Flynn, and M. A. Duncan, Int. J. Mass. Spectrom. **269**, 55 (2008).
[45] A. C. Scott, J. W. Buchanan, N. D. Flynn, and M. A. Duncan, Int. J. Mass. Spectrom. **266**, 149 (2007).
[46] A. C. Scott, N. R. Foster, G. A. Grieves, and M. A. Duncan, Int. J. Mass. Spectrom. **263**, 171 (2007).
[47] A. Simon and C. Joblin, J. Phys. Chem. A **111**, 9745 (2007).
[48] R. Takegami, a. Hosoya, J.-i. Suzumura, K. Yada, A. Nakajima, and S. Yabushita, Chem. Phys. Lett. **403**, 169 (2005).
[49] R. Takegami, N. Hosoya, J.-i. Suzumura, A. Nakajima, and S. Yabushita, J. Phys. Chem. A **109**, 2476 (2005).
[50] Y. Wang, J. Szczepanski, and M. Vala, Chem. Phys. **342**, 107 (2007).
[51] M. Welling, R. I. Thompson, and H. Walther, Chem. Phys. Lett. **253**, 37 (1998).
[52] K. F. Willey, P. Y. Cheng, M. B. Bishop, and M. A. Duncan, J. Am. Chem. Soc. **113**, 4721 (1991).
[53] K. F. Willey, C. S. Yeh, D. L. Robbins, and M. A. Duncan, J. Phys. Chem. **96**, 9106 (1992).
[54] W. Zheng, J. M. Nilles, O. C. Thomas, and K. H. Bowen, Chem. Phys. Lett. **401**, 266 (2005).
[55] W. Zheng, J. M. Nilles, O. C. Thomas, and K. H. Bowen, J. Chem. Phys.

**122**, 044306 (2005).

[56] A. K. Kandalam, B. K. Rao, P. Jena, and R. Pandey, J. Chem. Phys. **120**, 10414 (2004).

[57] R. Pandey, B. K. Rao, P. Jena, and M. A. Blanco, J. Am. Chem. Soc. **123**, 3799 (2001).

[58] R. Pandey, B. K. Rao, P. Jena, and J. M. Newsam, Chem. Phys. Lett. **321**, 142 (2000).

[59] B. K. Rao and P. Jena, J. Chem. Phys. **117**, 5234 (2002).

[60] B. K. Rao and P. Jena, J. Chem. Phys. **116**, 1343 (2002).

[61] L. Senapati, S. K. Nayak, B. K. Rao, and P. Jena, J. Chem. Phys. **118**, 8671 (2003).

[62] X. Zhang and J. Wang, J. Phys. Chem. A **112**, 296 (2008).

[63] F. Rabilloud, D. Rayane, A. R. Allouche, R. Antoine, F. Aubert-Frecon, M. Broyer, I. Compagnon, and Ph. Dugourd, J. Phys. Chem. A **107**, 11347 (2003).

[64] S. Kambalapalli and J. V. Ortiz, J. Phys. Chem. A **108**, 2988 (2004).

[65] J. Wang and J. Jellinek, J. Phys. Chem. A **109**, 10180 (2005).

[66] J. Zhou, W.-N. Wang, and K.-N. Fan, Chem. Phys. Lett. **424**, 247 (2006).

[67] K. M. Wedderburn, S. Bililign, M. Levy, and R. J. Gdanitz, Chem. Phys. **326**, 600 (2006).

[68] A. Goto and S. Yabushita, Chem. Phys. Lett. **454**, 382 (2008).

[69] X. Li, S. N. Eustis, K. H. Bowen, A. K. Kandalam, and P. Jena, J. Chem. Phys. **129**, 074313 (2008).

[70] X. Li and K. H. Bowen (unpublished).

[71] X. Li, S. N. Eustis, K. H. Bowen, and A. K. Kandalam, J. Chem. Phys. **129**, 124312 (2008).

[72] M. J. Frisch, G. W. Trucks, H. B. Schlegel *et al.*, GAUSSIAN 03, Revision C.02, Gaussian, Inc., Wallingford, CT, 2004.

[73] A. D. Becke, Phys. Rev. A **38**, 3098 (1988).

[74] J. P. Perdew and Y. Wang, Phys. Rev. B **45**, 13244 (1992).